Excitons in superlattices: Absorption asymmetry, dimensionality transition, and exciton localization

Norbert Linder
Institut für Technische Physik I, Universität Erlangen-Nürnberg, Erwin-Rommel-Straße 1, 91058 Erlangen, Germany
(Received 6 November 1996)

We calculate the field-dependent excitonic absorption spectra of semiconductor superlattices by diagonalizing the full Hamiltonian of the problem. Our model therefore includes both bound and continuum states of the excitons. The theoretical results are compared with experiments. We first show that the Coulomb interaction does not destroy the field-induced transition from the Franz-Keldysh to the Wannier-Stark regime, but causes an absorption asymmetry in the spectra, i.e., a dominance of Wannier-Stark transitions with negative indices. This effect, which has been observed before, is explained by a Coulomb-induced shift of oscillator strength from higher to lower energies in a simple model involving an effective Coulomb potential. We further address the problem of the transformation of the quasi-two-dimensional excitons of the Wannier-Stark levels to the three-dimensional miniband excitons obtained for zero field. For finite electric fields the quasibound miniband exciton states are explained as resonant states of the various Wannier-Stark excitons. We show that in contradiction to previous assumptions the Wannier-Stark ladder transitions are never suppressed by exciton localization. The *observability* of the transitions only depends on the relation between the zero-field miniband width and the linewidth of the transitions, but not on the ratio between miniband width and exciton binding energy. [S0163-1829(97)01820-1]

I. INTRODUCTION

For years, strongly coupled semiconductor superlattices have been investigated extensively, as they provide insight into certain new areas of solid-state physics which cannot be accessed in conventional crystals. The reason for this is that the precise control of layer thickness and material composition in epitaxial growth facilities allows one to fabricate artificial crystals with one-dimensional bands (minibands), the widths of which are tunable in a nearly arbitrary range. Additionally, well-established and sufficiently simple theoretical models allow for a comprehensive description of the electronic and optical properties of such structures, making a detailed comparison with experiment possible.

The first observation of the Wannier-Stark (WS) ladder in optical-absorption spectra[1,2] of semiconductor superlattices finished a long-lasting discussion about the formation of discrete (more exactly, quasidiscrete) energy levels when an electric field F is applied to an insulating crystal. This effect was proposed in the early days of solid-state physics,[3–5] but there has been no reliable observation in bulk crystals. In a semiclassical picture the finite widths of the bands force the electrons to fulfill coherent oscillations (Bloch oscillations) between the lower and upper band edges if tunneling between different bands and scattering processes can be neglected. The quantum-mechanical counterpart of this motion is a set of levels with a constant energy spacing eFd (d is the superlattice period) [Fig. 1(a)]. In the absorption spectra a corresponding series of equidistant transitions with quasi-two-dimensional character is obtained [Fig. 1(b)]. It is strikingly different from the Franz-Keldysh (FK) effect, which is well known for the field-dependent optical properties of bulk crystals.[6,7] The latter assumes infinitely extended energy bands, and leads to a continuous spectrum of eigenstates and transition energies, the oscillator strength of which yields characteristic oscillations in the absorption spectra. The FK effect was also expected to be obtained for low fields in the absorption spectra of superlattices, and was observed in 1991.[8,9] Later, the coexistence of both effects in the same structure was demonstrated,[10] and a consistent explanation of both effects was given, showing that the FK effect basically consists of an intensity modulation of the WS transitions.[11]

In the single-particle picture of Ref. 11, the transition from the WS to FK regimes is governed by the relation between the energetic distance and the linewidth of the WS transitions: For a decreasing field, WS transitions can only be observed as long as their spacing still exceeds the linewidth. Below, only the FK-type modulation of the WS transitions remains, which usually varies more slowly with the photon energy. The presence of the Coulomb interaction, however, adds a further physical quantity to the system, the relevant Coulomb energies, which can roughly be estimated in magnitude by the exciton binding energy. If the miniband widths are much larger, one expects the Coulomb effects to be relatively weak, affecting the structures in the absorption spectra only slightly. As the miniband widths become comparable to or even less than the exciton binding energy, however, significant changes in the spectra may occur. Specifically, the question arises as to how the Coulomb forces affect the transition from the WS to the FK regimes, and the formation of FK oscillations and the miniband exciton as the field decreases.

This problem can also be seen from a different point of view. The single-particle WS wave functions are spatially localized within a distance that is roughly equal to the semiclassical Bloch oscillation width Λ, i.e., $\Lambda=\Delta/(eF)$, where Δ is the miniband width. Thus a field F transforms the zero-field Bloch states, which are ''infinitely'' extended (in an

 © 1997 The American Physical Society

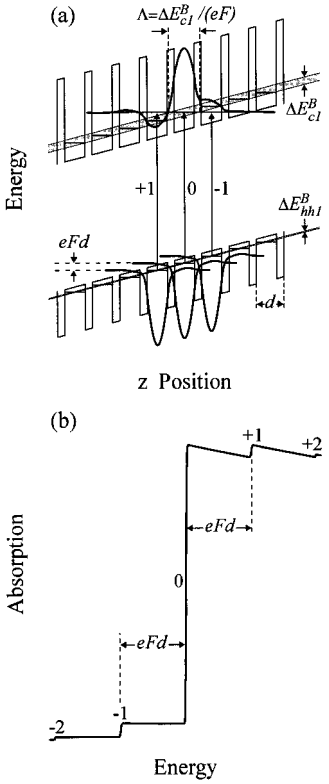

FIG. 1. Schematic drawing of (a) potential profile and a selection of WS states and (b) single-particle absorption spectra of a semiconductor superlattice with an electric field applied parallel to the growth direction. The shaded areas show the lowest conduction (c1) and uppermost heavy hole (hh1) miniband. Possible light-induced transitions are indicated by arrows in (a).

ideal superlattice) both in superlattice and in-plane direction, to the eigenstates of the WS ladder, which have ever-decreasing extension in the superlattice direction with increasing field.[12] In this way a transition from three-dimensional to quasi-two-dimensional behavior takes place. This kind of localization effect competes with an exciton localization mechanism, tending to move electrons and holes as close to each other as possible. One has to be aware, however, that the former is a single-particle effect, whereas the latter affects the two-particle system of electron and hole. The question is whether there is a turnover from one to the other effect as the field is decreased. This would imply that there might be a Coulomb-induced rearrangement of the sequence of WS transitions for low fields, accompanied by level anticrossings for increasing field. Actually, the theoretical results of Dignam and Sipe,[13,14] and the measurements of Fox *et al.*,[15] seem to indicate such a kind of behavior, but we will show below that a different interpretation appears to be more appropriate.

There have been a couple of theoretical approaches to calculate the excitonic absorption properties of strongly coupled superlattices. A large part of these were devoted to a discussion of exciton binding energies and oscillator strengths in the zero-field case,[16–18] mostly focusing on the change of dimensionality as a function of the superlattice period. Another topic has been the field dependence of the exciton energies and oscillator strengths,[19] which has been most extensively discussed by Dignam and Sipe.[13,14] These calculations, however, only took into account localized exciton states, and did not include the interaction with the excitonic continuum, which is essential for the low-field limit and a correct description of absorption spectra. The latter was achieved by Chu and Chang,[20,21] Whittaker,[22–24] and Glutsch, Chemla, and Bechstedt,[25] but their results were focused more on other aspects of the problem than those discussed here.

Our approach is based on Ref. 26. We outline the theory and the modifications necessary to deal with our problem in Sec. II. In Sec. III we discuss basic aspects of the absorption spectra, and give some interpretation of previous experimental results. In Sec. IV we develop a simple picture for the excitonic absorption asymmetry of WS transitions with positive and negative indices. Section V contains a comparison between calculated and experimental absorption spectra for a wide-miniband superlattice, focusing on the transition between FK and WS regimes. The details of the field-induced three-dimensional (3D)-to-2D transition of the exciton states and the exciton localization will be discussed in Sec. V. Finally, we summarize our results.

II. THEORY

For the calculations we assume an infinite superlattice with an ideal rectangular shape of the coupled potential wells. In the effective-mass approximation (EMA) the Wannier equation for the two-particle envelope function $\Psi^{\epsilon^x}(\vec{r}_e,\vec{r}_h)$ reads

$$\left(H_e(\vec{r}_e)+H_h(\vec{r}_h)-\frac{e^2}{4\pi\epsilon_0\epsilon_r|\vec{r}_e-\vec{r}_h|}\right)\Psi^{\epsilon^x}(\vec{r}_e,\vec{r}_h)$$
$$=(\epsilon^x-E_g)\Psi^{\epsilon^x}(\vec{r}_e,\vec{r}_h), \tag{1}$$

where

$$H_{e/h}(\vec{r}_{e/h})=-\frac{\hbar^2}{2m^*_{z,e/h}}\frac{\partial^2}{\partial z^2_{e/h}}-\frac{\hbar^2}{2m^*_{\parallel,e/h}}\frac{\partial^2}{\partial \vec{r}^2_{\parallel,e/h}}+V(z_{e/h}) \tag{2}$$

are the single-particle parts of the Hamiltonian, with $V(z_{e/h})$ the superlattice potential and $m^*_{z,e/h}$ and $m^*_{\parallel,e/h}$ the effective masses in the z and in-plane directions for electrons and holes, respectively.

For the in-plane direction the problem can be separated into center-of-mass and relative coordinates. In the dipole approximation, only excitons with vanishing center-of-mass momentum are optically active, and we will restrict our considerations to these states. The total Hamiltonian then becomes

$$H_{\rm eh}(\vec{\rho},z_e,z_h)=-\frac{\hbar^2}{2\mu_\parallel}\frac{\partial^2}{\partial\vec{\rho}^2}-\frac{\hbar^2}{2m^*_{z,e}}\frac{\partial^2}{\partial z_e^2}-\frac{\hbar^2}{2m^*_{z,h}}\frac{\partial^2}{\partial z_h^2}$$
$$+V(z_e)+V(z_h)-\frac{e^2}{4\pi\epsilon_0\epsilon_r\sqrt{(z_e-z_h)^2+\rho^2}}. \tag{3}$$

In the one-miniband approximation, neglecting tunneling between different minibands, the z-dependent part of the elec-

tron and hole eigenfunctions can be calculated using the crystal momentum representation.[4] One obtains

$$\xi_{n\nu}(z_{e/h})=\frac{\sqrt{d}}{2\pi}\int_{-\pi/d}^{+\pi/d}\exp\left\{\frac{i}{eF}\int_0^{k_z}[E_n(k_z')-E_{n0}]dk_z'\right\}$$
$$\times\exp\{ik_z(z_{e/h}-\nu eFd)\}u_{nk_z}(z)dk_z. \quad (4)$$

Here, $\xi_{n\nu}$ is the νth WS ladder state of miniband n, $E_n(k_z')$ the miniband dispersion, and $E_{n\nu}$ the energy of the WS level, given by

$$E_{n\nu}=E_{n0}+\nu eFd, \quad (5)$$

where

$$E_{n0}=\frac{d}{2\pi}\int_{-\pi/d}^{+\pi/d}E_n(k_z')dk_z'. \quad (6)$$

$u_{nk_z}(z)$ is the part of the miniband Bloch functions,

$$\phi_{nk_z}(z)=e^{ik_zz}u_{nk_z}(z), \quad (7)$$

which is periodic with the superlattice. We have calculated them using a Kronig-Penney model.[27] Below, we restrict ourselves to one pair of minibands and write $n=c/n=v$ for the respective conduction and valence miniband. The total Hamiltonian is then expanded in single-particle wave functions. The discrete translation invariance of the system in the z direction allows us to write the electron-hole product function in Bloch form,

$$\chi_{K_z,\eta}(z_e,z_h)=\frac{1}{\sqrt{N}}\sum_\nu e^{i\nu K_zd}\xi^*_{c,\nu+\eta}(z_e)\xi_{v,\nu}(z_h), \quad (8)$$

where $N\to\infty$ is the number of superlattice periods.

The total exciton envelope function now reads

$$\Psi^{\varepsilon^x}(\vec{r}_e,\vec{r}_h)$$
$$=\frac{\sqrt{A}}{(2\pi)^2}\sum_{K_z,\eta}\int k\,dk\,d\phi\,\Phi^{\varepsilon^x}_{K_z,\eta}(k)e^{-i\vec{k}\vec{\rho}}\chi_{K_z,\eta}(z_e,z_h). \quad (9)$$

Equations (8) and (9) are equivalent to a transformation in center-of-mass and relative coordinates on the scale of the superlattice period. In this sense, $\chi_{K_z,\eta}$ is the function for the relative motion and ηd is its (quasicontinuous) argument, since ηd describes the relative offset of electron and hole wave functions. K_z represents the exciton center-of-mass momentum, and can have the usual values between $-\pi/d$ and $+\pi/d$ with a spacing of $2\pi/Nd$.

The expansion coefficients $\Phi^{\varepsilon_x}_{K_z,\eta}(k)$ are assumed to be independent of the in-plane angle of the $\vec{k}$ vector, since only states with s-like in-plane symmetry contribute to the optical absorption in the EMA.[26] It should be mentioned that this result is also obtained for the total angular dependence of the exciton wave functions resulting from a full $\vec{k}\cdot\vec{p}$ calculation.[28]

One major advantage of our basis is that the exciton Hamiltonian becomes diagonal with respect to K_z. Furthermore, in the dipole approximation, only states with $K_z=0$ are optically active, i.e., the k-conservation rule is obtained similarly as in bulk material (as long as the superlattice period is small compared to the wavelength of the incident light). This can easily be seen from a calculation of the optical matrix element, which contains the overlap integral of electron and hole basis states:

$$\sum_\nu e^{i\nu K_zd}\int\xi^*_{c,\nu+\eta}(z_e)\xi_{v,\nu}(z_h)\,dz$$
$$=\sum_\nu e^{i\nu K_zd}\int\xi^*_{c,\eta}(z_e)\xi_{v,0}(z_h)\,dz$$
$$=N\delta_{K_z,0}\int\xi^*_{c,\eta}(z_e)\xi_{v,0}(z_h)\,dz. \quad (10)$$

In the first line, the translation invariance of the Kane functions has been used. Hence, for the calculation of optical-absorption spectra, only the $(K_z=0)$ states have to be taken into account, which amounts to a reduction of the problem from three to two independent dimensions.

The evaluation of the Hamilton matrix elements is straightforward. One finally finds a system of integral equations for the coefficients $\Phi^{\varepsilon^x}_{0,\eta}(k)$,

$$\left(E_c^0-E_v^0+\eta' eFd+\frac{\hbar^2k'^2}{2\mu_{cv,\parallel}}-\varepsilon^x\right)\Phi^{\varepsilon^x}_{0,\eta'}(k')-\frac{e^2}{8\pi^2\epsilon_0\epsilon_r}\sum_\eta\int k\,dk\,\Phi^{\varepsilon^x}_{0,\eta}(k)\int d\phi\int dz_e dz_h\,\frac{e^{-|\vec{k}'-\vec{k}||z_e-z_h|}}{|\vec{k}'-\vec{k}|}$$
$$\times\sum_\nu\xi_{c,\eta'}(z_e)\,\xi^*_{v,0}(z_h)\,\xi^*_{c,\eta+\nu}(z_e)\,\xi_{v,\nu}(z_h)=0, \quad (11)$$

which can be discretized and transformed to an eigenvalue equation in matrix form. Since there are no presumptions made about the shape of the wave functions, the approach contains both bound and continuum states of the excitons. After diagonalization, the absorption is obtained from the eigenvalues ε^x and the coefficients $\Phi^{\varepsilon^x}_{0,\eta}(k)$ according to

$$\alpha(\omega)=\frac{\pi e^2}{\epsilon_0m_0^2cn_{\rm opt}L}\frac{1}{(2\pi)^2}|\hat{\vec{e}}\cdot\vec{p}_{cv}|^2\sum_{\varepsilon^x}\left|\sum_\eta\int k\,dk\,\Phi^{\varepsilon^x}_{0,\eta}(k)\int dz\,\xi^*_{c,\eta}(z)\xi_{v,0}(z)\right|^2\delta_\Gamma(\hbar\omega-\varepsilon^x). \quad (12)$$

Here L is the length of the sample, $n_{\rm opt}$ the refractive index, δ_Γ a broadened δ function, and $|\hat{\vec{e}}\cdot\vec{p}_{cv}|^2$ the polarization-dependent square of the bulk momentum matrix element given by

$$|\hat{\vec{e}}\cdot\vec{p}_{cv}|^2=\begin{cases} P^2(e_x^2+e_y^2), & v=\text{hh} \\ \frac{1}{3}P^2(e_x^2+e_y^2)+\frac{4}{3}P^2e_z^2, & v=\text{lh} \\ \frac{2}{3}P^2, & v=\text{so}, \end{cases} \tag{13}$$

with P^2 taken from Ref. 29.

The numerical evaluation of the Eqs. (11) and (12) has been performed according to Ref. 26. The summation over the index ν in Eq. (11) terminates by itself, since the WS wave functions are well localized inside a range of z values, which is approximately given by

$$\frac{E_{n0}-E_n^l}{eFd}+\nu d\gtrsim z\gtrsim\frac{E_{n0}-E_n^u}{eFd}+\nu d, \tag{14}$$

where E_n^l and E_n^u are the lower and upper miniband edges.

For the same reason, the infinite integrals over z_e and z_h can be restricted to a well-defined finite range. Finally, only a finite set of states η has to be used in the expansion. The spatial extension of the WS wave functions, however, increases, as the field decreases. Consequently, a larger number of basis states has to be taken into account, which practically imposes a lower bound on the fields, for which precise results can be obtained. In particular, for the zero-field limit, a different approach has to be used.

Rather than the superlattice Bloch functions, which would be obtained in the zero-field limit, but are infinitely extended, the Wannier functions $a_{n,p}(z)$, defined by

$$a_{n,p}(z)=\frac{1}{\sqrt{N}}\sum_{k_z} e^{-ik_zpd}\phi_{nk_z}(z), \tag{15}$$

provide a more convenient basis for an expansion of the zero-field Hamiltonian, since they are strongly localized. Furthermore, they have the same symmetry properties as the Kane states, i.e.,

$$a_{n,p}(z)=a_{n,0}(z-pd). \tag{16}$$

Thus, if the envelope function is written in the form of the Eqs. (8) and (9), but with the Kane states replaced by electron and hole Wannier functions,

$$\chi^0_{K_z,\eta}(z_e,z_h)=\frac{1}{\sqrt{N}}\sum_{\nu} e^{i\nu K_zd}a^*_{c,\nu+\eta}(z_e)a_{v,\nu}(z_h), \tag{17}$$

the situation is analogous to the above case of a nonzero field. The single-particle part of the exciton Hamiltonian, however, is no longer diagonal in η, but becomes equal to

$$\sum_\eta\left[\frac{d}{2\pi}\int_{-\pi/d}^{+\pi/d}E_{cv}(k_z)e^{ik_z(\eta-\eta')d}dk_z+\left(\frac{\hbar^2k'^2}{2\mu_{cv}}-\varepsilon^x\right)\delta_{\eta\eta'}\right]\Phi^{\varepsilon^x}_{0,\eta}(k'), \tag{18}$$

i.e., it contains the Fourier components of the combined miniband dispersion. In the case of tight-binding minibands, the only off-diagonal terms are obtained for $|\eta-\eta'|=1$ (which are equal to one half of the combined miniband width, $\Delta E^B_{cv}/2$), but for a more realistic dispersion, higher-order terms occur as well. Using Eq. (18) and the Coulomb matrix elements defined as before, the Hamilton matrix can be calculated, and the further procedure is completely equivalent to the case of a nonvanishing field.

In a superlattice structure satisfying inversion symmetry for zero field, a further reduction of the complexity of the problem can be achieved, if the latter symmetry is exploited. For this reason, completely symmetric and antisymmetric basis states can be formed by

$$\chi^{\pm}_{0,\eta}=\begin{cases} \frac{1}{\sqrt{2}}[\chi^0_{0,\eta}(z_e,z_h)\pm\chi^0_{0,-\eta}(z_e,z_h)], & \eta\neq 0 \\ \chi^0_{0,0}(z_e,z_h), & \eta=0,\text{``}+\text{''} \\ 0, & \eta=0,\text{``}-\text{''}. \end{cases} \tag{19}$$

The exciton Hamiltonian, which is invariant under the inversion, does not mix symmetric (``+'') and antisymmetric (``−'') states. Using the properties of the Wannier functions, it is easy to show that only the symmetric states have a nonvanishing optical matrix element, i.e., are responsible for the optical absorption. The exciton Hamiltonian can, therefore, be expanded in terms of the symmetric eigenstates, which allows us to reduce the order of the corresponding matrix to its half plus one without any loss of relevant information.

III. BASIC ABSORPTION CHARACTERISTICS

Below we restrict ourselves to the lowest pair of heavy-hole (hh) and conduction (c) minibands. The most interesting case is, when the combined hh1-c1 miniband width is of the order of the exciton binding energies. Then, the system is between the quasi-2D limit of a multiple quantum well (MQW) structure, where the exciton energies are larger than the miniband widths, and the 3D wide-band limit of bulk material. For this reason, a superlattice structure, consisting of 12-ML GaAs wells and 6-ML AlAs barriers has been chosen as a theoretical example, since the combined hh1-c1 miniband width $\Delta E^B_{\rm hh1,c1}=22.8$ meV is both beyond the 3D ($\varepsilon^x_0\approx 4$ meV) and the exactly 2D ($\varepsilon^x_0\approx 16$ meV) binding energies of GaAs, but not too far.

Figure 2(a) shows a set of calculated excitonic absorption spectra over a wide range of the electric field. In the calculations, a finite Gaussian broadening with a full width at half maximum (FWHM) of 3 meV has been used. For comparison, the corresponding spectra of the derivative $\partial\alpha/\partial\omega$ of the absorption without the Coulomb interaction is plotted in Fig. 2(b).

For high fields WS transitions can clearly be resolved as excitonic peaks in Fig. 2(a) [marked with (x)], accompanied by the onset of the corresponding absorption continuum, including the dense quasicontinuum of higher bound states, (c) on the high-energy side. Similar peaks are obtained in the single-particle differential absorption spectra of Fig. 2(b), resulting from the differentiation of the WS absorption steps.

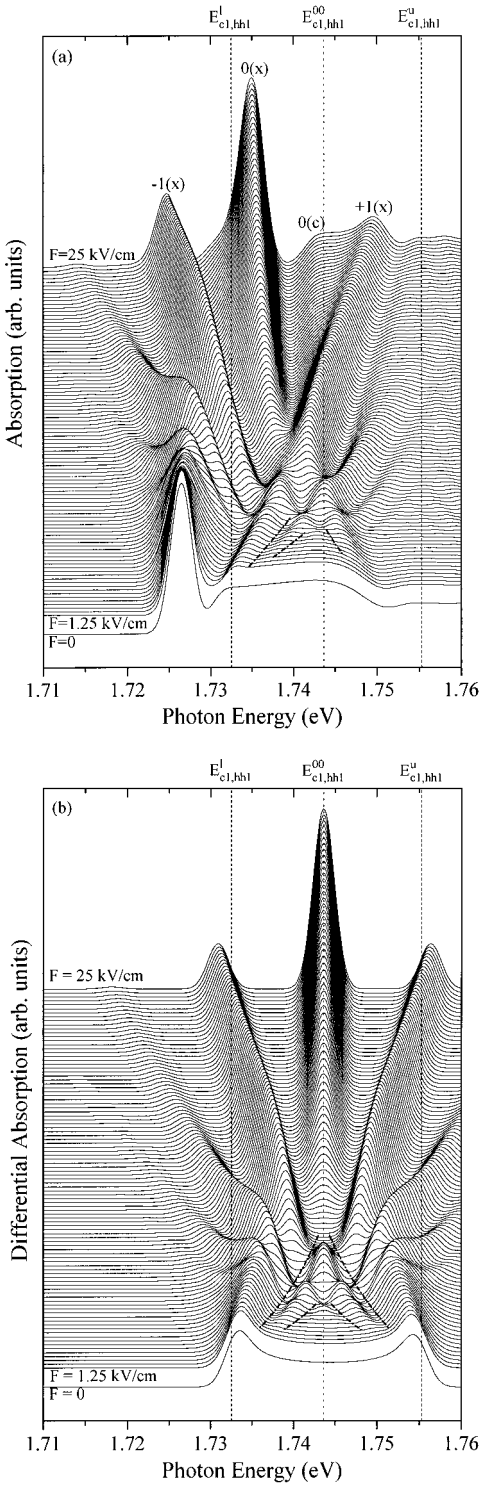

FIG. 2. (a) Excitonic absorption spectra and (b) single-particle spectra of the differential absorption of the 12/6-ML GaAs/AlAs superlattice at $T=77$ K for a wide range of electric fields. The dash-dotted lines indicate the positions of the FK oscillation minima.

In this field range the transitions are clearly 2D in character. For decreasing field, however, the energetic distance between the WS transitions falls below the value of the broadening parameter and individual peaks can no longer be resolved. At this point ($F \lesssim 10$ kV/cm, intermediate fields) the interplay of bound and continuum exciton states combined with varying oscillator strengths makes an unambiguous identification of individual structures impossible. Gradually, however, the structures in the spectra transform to a pattern which is characteristic for FK oscillations (low fields). In particular, for energies in the range of the combined miniband, regular structures of maxima and minima are formed which move toward the miniband edges (indicated by dash-dotted lines in Fig. 2). This generalized FK behavior has been described in detail for the single-particle absorption.[11] Remarkably, it is not destroyed by the presence of the Coulomb interaction, even if the distance between neighboring FK maxima is much less than the exciton binding energy. All structures as a whole, however, are shifted to lower energies, due to the attractive character of the Coulomb interaction. In this field and energy range the absorption spectra are dominated by the properties of the single-particle states, and the Coulomb interaction mainly adds a smooth modulation, at least for the continuum states. This is also reflected in the strong resemblance between the spectra of Figs. 2(a) and 2(b).

In the zero-field limit, the spectrum consists of an exciton peak and a broad plateau, rising at the lower single-particle miniband gap. Some meV below the upper combined miniband edge, the absorption drops off, has a slight dip, and reaches a mostly constant value at the energy of the upper miniband edge. These are the characteristics of a 3D absorption spectrum, consisting of M_0 and M_1 critical points. The exciton state near the lower miniband edge has a binding energy of 6.25 meV, which is larger than that of bulk GaAs ($\varepsilon^x \approx 4.1$ meV), because the electron-hole dispersion is strongly anisotropic. At the upper miniband edge, the weak absorption maximum, followed by the dip, is the signature of the lowest bound-state resonance of the M_1 exciton. This kind of structure was predicted by Kane[30] and Balslev.[31] The finite numerical discretization prevents a finer resolution of the spectra in our calculations, but similar structures have been extensively discussed by Whittaker[24] and Glutsch, Chemla, and Bechstedt.[25]

The preceding discussion has shown that at least in the intermediate-to-low-field range a detailed analysis of the absorption spectra requires a series of consecutive spectra to make a definite identification of the structures possible. In order to illustrate this, we investigate experimental results of Agulló-Rueda *et al.*,[32] and restrict ourselves to the hh1-c1 transitions as before. In Fig. 1 of their paper, these authors plotted photocurrent spectra of a (40 Å/40 Å) GaAs/$Al_{0.35}Ga_{0.65}As$ superlattice for two different values of the electric field. The lower spectrum is in the high-field limit ($F \approx 40$ kV/cm), where only the ($\eta=0$) transition can be observed, whereas the upper spectrum corresponds to an intermediate-field situation ($F \approx 10$ kV/cm), since two WS peaks can clearly be identified ($\eta=-1$ and 0). In this spectrum, however, an additional small hump can be seen at slightly higher energies, which was attributed to the onset of the continuum above the ($\eta=0$) exciton peak. The authors, however, could not explain the peak shape of this structure, since they expected to find a shoulder as usual for quasi-2D exciton spectra, and as observed in the high-field spectrum. In Fig. 3, a set of calculated spectra for the same sample is shown. One recognizes that at $F=10$ kV/cm a similar shape of the absorption is obtained, exhibiting, in particular, a

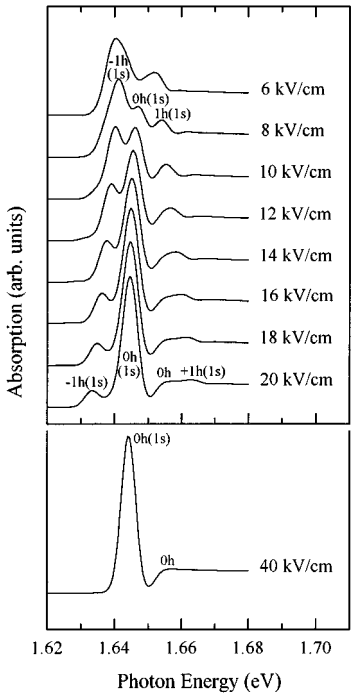

FIG. 3. Calculated excitonic electroabsorption spectra of a (40 Å/40 Å) $GaAs/Al_{0.35}Ga_{0.65}As$ superlattice at 5 K as discussed in Ref. 33.

small high-energy peak above the (-1) and (0) exciton transitions. Now it is possible to trace the field dependence of this structure. One realizes that it becomes broader first, and finally splits into a pair of structures: a low-energy shoulder, marking the onset of the continuum, and a small peak, which is identified as the $(+1)$ exciton transition owing to its field dependence. Obviously, the hump at 10 kV/cm contains both of these, being the reason for its unusual shape. The further development to lower fields shows that the spectral resolution is not enough to decompose this structure into excitonic peaks again, but that it transforms gradually to the upper edge of the zero-field absorption continuum.

IV. EXCITON ASYMMETRY

In Fig. 2 a strong asymmetry between $-\eta$ and $+\eta$ transitions can be observed in the excitonic spectra. This is nearly completely absent in the single-particle spectra, which would be exactly symmetric with respect to the $(\eta=0)$ transition in the case of a symmetric (i.e., tight-binding-like) miniband dispersion. This excitonic asymmetry has been obtained before by Dignam and Sipe.[14] Their calculations, however, were based on a consideration of bound exciton states only, using a variational principle. We obtain similar results, demonstrating that the Coulomb forces generally redistribute oscillator strength from states of higher energy to states of lower energy. This effect can be explained in a rather intuitive picture.

For simplicity, we assume a superlattice with a quasicontinuous translation symmetry, which allows us to separate the center-of-mass motion from the relative motion of the electron-hole pair. Then the kinetic part of the relative electron-hole motion is determined by the combined miniband dispersion $E_{c1,hh1}(k_z)=E_{c1}(k_z)-E_{hh1}(k_z)$ for the z direction, and the reduced effective mass for the direction parallel to the layers. The potential energy is given by the electric-field term eFz and the Coulomb term $e^2/4\pi\epsilon_0\epsilon_r\sqrt{\rho^2+z^2}$, where $z=z_e-z_h$ and $\vec{\rho}=\vec{r}_{e,\parallel}-\vec{r}_{h,\parallel}$ are the relative coordinates. Next we want to consider the lowest bound exciton states of the electron-hole WS ladder, and assume that the exciton envelope function $\Psi^x_\eta(\vec{\rho},z)$ can be separated in a part $f^x_\eta(z)$ for the z direction and a part parallel to the layers, which has the form of the lowest bound state of a 2D exciton,[33] $g^x_\eta(\vec{\rho})=(4/a_x)\exp(-2\rho/a_x)$, yielding

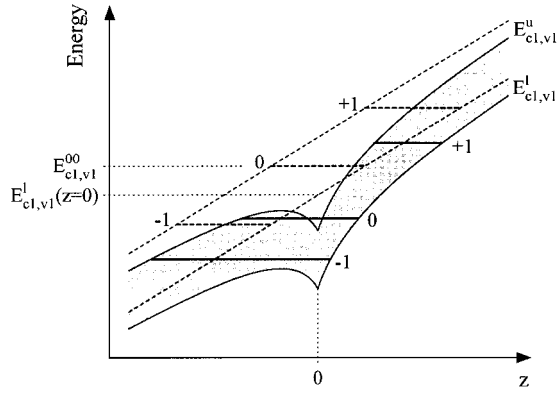

FIG. 4. Effective miniband structure for the relative electron-hole motion, with (shaded area) and without (dashed lines) the effective Coulomb potential. For both cases, three electron-hole (exciton) WS levels are plotted schematically.

$$\Psi^x_\eta(\vec{\rho},z)=f^x_\eta(z)g^x_\eta(\vec{\rho})=\frac{4}{a_x}\,e^{-2\rho/a_x}f^x_\eta(z), \tag{20}$$

with an effective Bohr radius a_x for the in-plane wave function. The effective Bohr radius is, in principle, a function of the WS ladder index η, but we will assume this dependence to be negligible. Calculating the expectation value with respect to the in-plane motion leads to a positive energy constant $\varepsilon_\parallel$ contributing to the kinetic energy. The electric-field term eFz remains unaffected, and the Coulomb term is replaced by

$$V^{\rm eff}_{\rm Coul}(z)=\frac{16}{a_x^2}\int\frac{e^2}{4\pi\epsilon_0\epsilon_r\sqrt{z^2+\rho^2}}\,e^{-4r/a_x}d^2\vec{\rho}. \tag{21}$$

The integral can be transformed to

$$V^{\rm eff}_{\rm Coul}(z)=\frac{4e^2}{a_x\epsilon_0\epsilon_r}\left\{2\int_0^\infty e^{-2x}\left[x^2+\left(\frac{2z}{a_x}\right)^2\right]^{1/2}dx-\left|\frac{2z}{a_x}\right|\right\}, \tag{22}$$

and is now expressed in terms of the reduced z coordinate $2z/a_x$.

The relative motion of the exciton in the z direction is now determined by the combined miniband width and an effective potential $eFz+V^{\rm eff}_{\rm Coul}(z)$. This is shown schematically in Fig. 4, where the effective combined miniband structure with (shaded areas) and without (area between the

dashed lines) the Coulomb interaction is drawn. The singularity of the Coulomb potential has disappeared due to the 2D integration over the in-plane part of the wave function, but a kink at $z=0$ remains.

Now it is possible to discuss the behavior of the z part of the exciton wave functions. An example of three (equidistant) WS levels $\eta=-1$, 0, and $+1$ without the Coulomb interaction is drawn schematically as the horizontal dashed lines in Fig. 4. The corresponding exciton levels are plotted as solid lines, where it is assumed that the exciton binding energy is the same for $\eta=+1$ and -1, and larger for $\eta=0$. The striking point, now, is that the exciton probability density is mostly confined within the spatial range inside the combined miniband, i.e., the shaded area. The exciton oscillator strength, however, is proportional to the probability density at $z=0$. Thus it is obvious that the $\eta=-1$ state (and any state $\eta<0$ slightly below $E^{l}_{\mathrm{c1,h1}}$) has a higher absorption probability than the $\eta=+1$ state, since the spatial extension of the $\eta=-1$ exciton wave function covers the point $z=0$, whereas the $\eta=+1$ wave function only has a small tail at $z=0$, resulting from tunneling into the energy gap above the upper combined miniband edge.

The above considerations do not rely on the exact shape of the effective Coulomb potential $V^{\mathrm{eff}}_{\mathrm{Coul}}$. Obviously, it is sufficient to have a potential which is symmetric with respect to $z=0$, and has a distinct minimum there. Both properties remain fulfilled in a more realistic description of the problem.

V. FK AND WS EFFECTS: COMPARISON WITH EXPERIMENT

In Fig. 2, it has been shown that, in spite of the Coulomb forces tending to localize the electron and hole close to each other, the interplay between WS transitions and FK oscillations is not suppressed, although the width of the FK oscillations can become less than the exciton binding energy. In a wide-miniband superlattice, which is closer to a 3D system, the FK effect has been observed experimentally, and it has been shown that a single-particle theory accounts well for the basic structures.[11] The line shapes and the intensity of the structures, however, were found to be different, and we will show in this section that this is due to the excitonic effects.

In Fig. 5, experimental absorption spectra obtained from a photocurrent measurement for a 11/1-ML GaAs/AlAs superlattice are compared with calculated spectra with and without the Coulomb interaction. The structure and the experimental details were described in detail in Ref. 11. For the calculations, only the hh1-c1 transitions have been taken into account, an approximation, whose validity was also discussed in Ref. 11. An energy- and field-dependent Gaussian broadening function has been used with a base value of the FWHM equal to 20 meV at $F=0$ and $\hbar\omega=1.5$ eV, which increases by a factor of 2 both between 1.5 and 2.1 eV, and from $F=0$ to 250 kV/cm (hence, at $F=250$ kV/cm and $\hbar\omega=2.1$ eV the value of the FWHM is 80 meV), and is kept constant above these values. The field and energy dependence of the broadening are used to give agreement with the experimental values. The complexity of the numerical calculations comes to the limits of the available computing capacities; for the lowest displayed field value ($F=33$ kV/cm), a matrix larger than 5000 by 5000 had to be diagonalized, and the further increase of the number of WS states, which would be necessary to calculate for lower field values, prevents us from closing the gap between $F=33$ kV/cm ($U_{pn}=+0.85$ V) and $F=0$ ($U_{pn}=+1.75$ V).

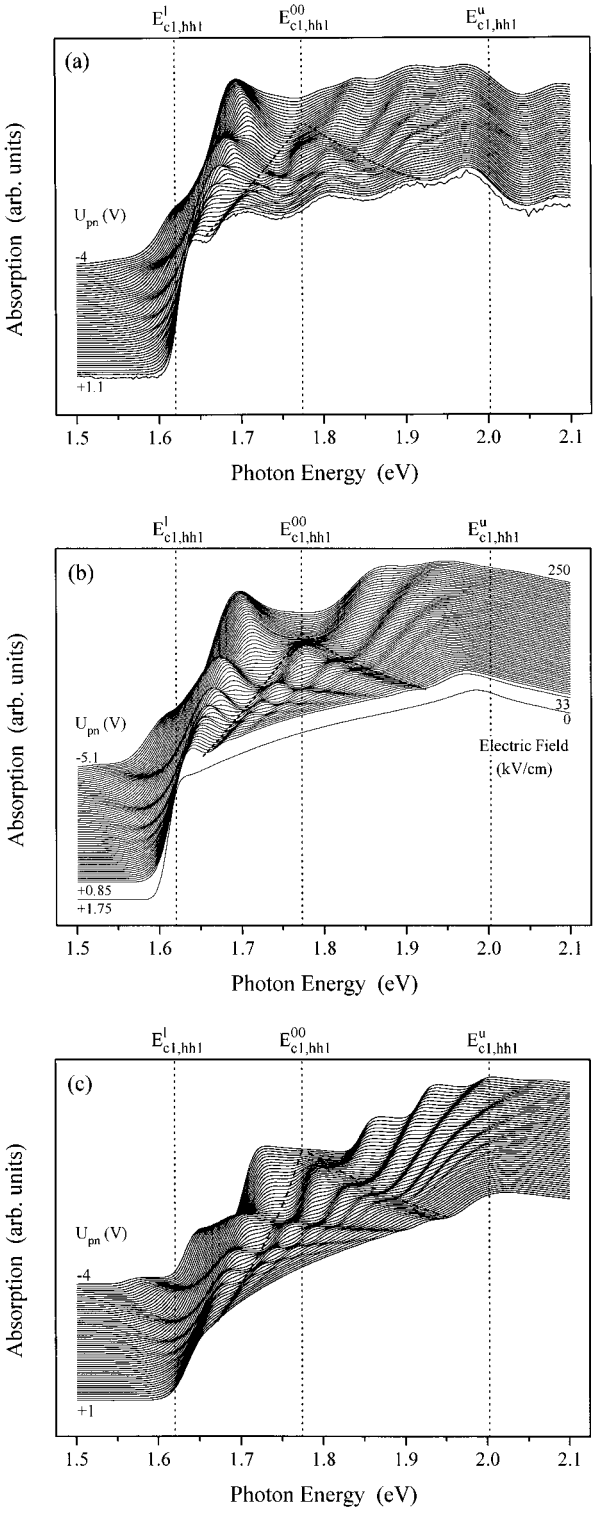

FIG. 5. Field-dependent experimental (a) and theoretical excitonic (b) and single-particle (c) absorption spectra for a 11/1-ML GaAs/AlAs superlattice at $T=77$ K. The dashed lines indicate the region of coexistence of the WS and FK effects for the c1-hh1 transitions.

Nevertheless, the agreement between theory and experiment is nearly perfect. As in experiment, the smooth increase of the single-particle absorption [Fig. 5(c)] at the fundamental gap is replaced by a steplike structure. The slope is only determined by the line broadening, which also shifts the absorption feature of the M_0 exciton to a value slightly above the band-gap energy. A high-resolution calculation, however, shows that actually a bound exciton state with a binding energy of about 5 meV exists. For higher energies, both theory and experiment yield a slightly increasing absorption plateau between the M_0 and M_1 points of the combined density of states. Near the saddle point, the theoretical spectra drop off, but they do not exhibit the absorption dip expected for the M_1 exciton, due to the large line broadening. The experimental spectra seem to have an even more pronounced saddle-point feature, but it is more likely that the apparent decrease of the absorption, which actually is a decrease of the measured photocurrent, results from the onset of the absorption in an $Al_{0.45}Ga_{0.55}As$ cladding layer, grown on top of the superlattice structure, which does not contribute to the photocurrent.

Both FK oscillations and WS transitions can clearly be identified, and the line shapes agree very well. The vertex of the triangular section of coexistence of FK and WS effects (dashed lines) appears at a higher field value in the theoretical spectra, indicating that the actual combined miniband width is somewhat smaller than calculated. Figure 6 shows the results of doubly differential photocurrent (DDPC) spectra, and the corresponding calculated spectra of $\partial^2\alpha/\partial F\partial\omega$. Since the constant part of the photocurrent (absorption) is suppressed in these spectra, the field- and wavelength-dependent structures can be observed much more clearly than in Fig. 5. Here the interplay of FK and WS effects in the triangular section can clearly be identified. In comparison with a plot of similar spectra without the Coulomb interaction[11] the predicted Coulomb enhancement of the structures in the lower half of the miniband becomes prominent.

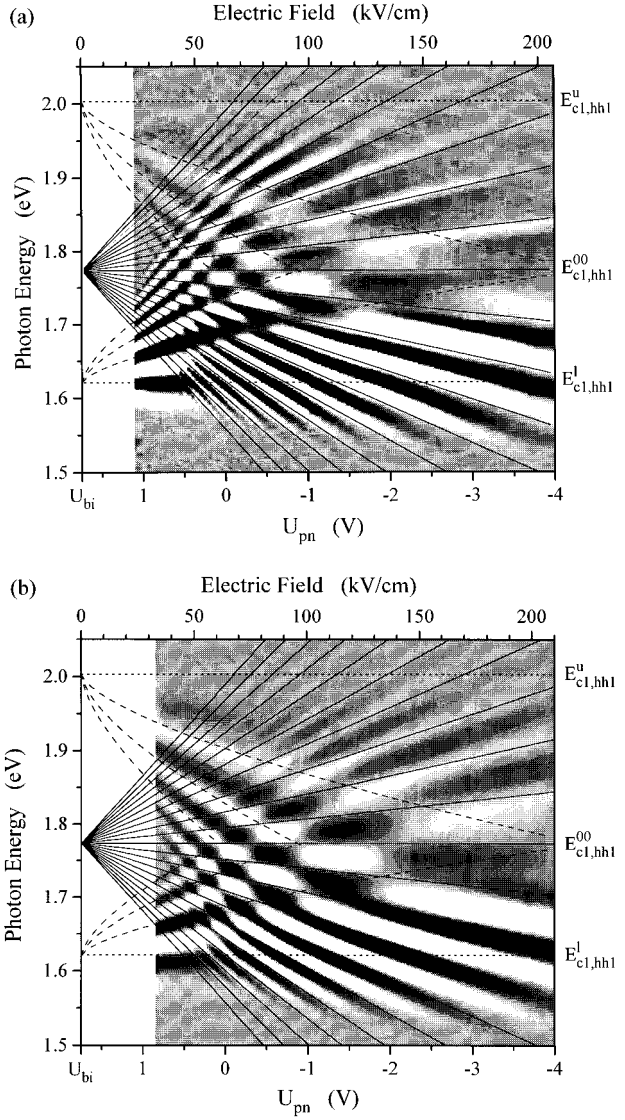

FIG. 6. (a) Gray scale plot of DDPC spectra and (b) calculated excitonic $\partial\alpha^2/\partial\omega\partial F$ spectra for the 11/1 GaAs/AlAs superlattice. In both plots the theoretical fan of single-particle WS transitions (solid lines) and FK oscillations (dashed lines), and the combined miniband edges (dotted lines) are included.

VI. FIELD-INDUCED TRANSITION FROM 3D TO 2D ABSORPTION CHARACTER

An electric field provides an excellent tool to study the transition from 3D to 2D character in a superlattice, since it can shrink the electronic wave functions from a quasi-infinite extension to values of the order of one superlattice period. The situation in the presence of excitonic effects becomes more difficult. The problem is that one is used to thinking of an exciton as a quasiparticle. In this picture, there exists a hydrogenlike 3D two-particle system in the zero-field limit, which has a series of bound states with finite spatial extension, and a continuum of infinitely extended quasifree states (Fig. 7). As a weak electric field is applied, the bound states are ionized into the continuum with a certain transition probability. As a consequence, the lifetime of the bound states is reduced, and the corresponding absorption peaks gain additional width, as soon as the ionization time falls below the ''natural'' lifetime. Yet the character of the particle does not change, and remains 3D. This is also the situation for bulk material, where an electric field leads to suppression of the excitonic absorption peak and eventually even to the disappearance of quasibound exciton levels, resulting in the formation of the FK absorption tail and FK oscillations.

In the superlattice, however, the high-field situation is characterized by the existence of a series of exciton states, each belonging to one pair of electron and hole WS levels. At this point, we have to emphasize the results of the preceding sections and Ref. 11, where it was proved that these states do not evolve from FK oscillations, being the high-field signature of a 3D system. Instead, these states are 2D in character, each having its own series of bound and continuum exciton states, part of which could be seen, e.g., in Fig. 2. The corresponding excitons can be considered as quasi-2D particles, having a certain probability distribution in the third dimension (the superlattice direction). The latter, however, is the same for all states of the exciton, and this is the property that establishes the 2D character. Of course, there is a gradual transition from the 2D (high-field) limit to the 3D (zero-field) limit, as the calculations plotted in Fig.

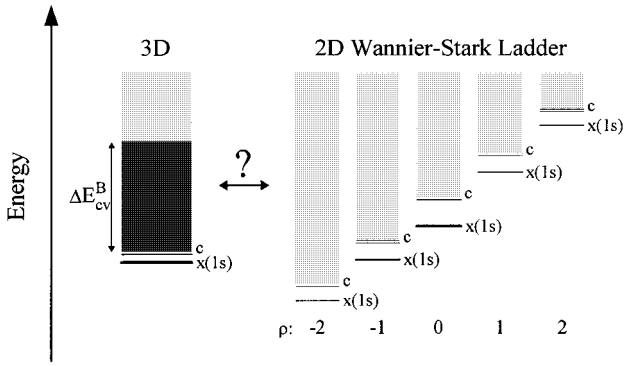

FIG. 7. 3D and 2D series of bound exciton states and exciton continua, corresponding to the zero- and the high-field limits of a superlattice. The line thickness of the bound levels gives an indication for the oscillator strength.

2(a) clearly prove. The question is to find a physical picture of the mechanisms involved and their consequences.

There is a variety of aspects to approaching this problem. From the view of mathematical formalism, there are two effects which influence the way the transition takes place. One is the Coulomb-induced mixing of the bound quasi-2D exciton states, in particular the mixing of the ground states, which was discussed in Ref. 14. The other consists of the interaction of the bound WS exciton states with the continuum of lower WS transitions. The latter leads to the formation of a Fano resonance for each exciton absorption peak. The width of the resonance depends on the Coulomb coupling between the discrete exciton levels and the underlying absorption continua, and increases as the field decreases. At the same time, the spacing of the WS levels decreases, and, as soon as it falls below the resonance broadening, the peaks of the WS excitons overlap and, eventually, become indistinguishable. This effect is mostly restricted to the energy range of the combined miniband, since both the WS absorption peaks and the absorption continua have large values in this range only, due to the localization of the single-particle states. In this way, the formation of the zero-field absorption plateau can be interpreted as the zero-field limit of superimposed resonance-broadened WS levels, and the absorption dip of the 3D saddle-point exciton as the result of the superimposed dips on the high-energy side of the Fano resonances. The resonance widths, however, are given immediately by the Coulomb matrix elements between the bound states and the continua,[34] an upper limit of which is certainly the exciton binding energy. Hence, to observe the proposed transition behavior experimentally, a spectral resolution far below this value will be necessary. This has not yet been achieved in actual experiments, where the transition behavior has always been governed by different broadening mechanisms.

The Fano resonance picture is not able to account for the formation of the bound states of the 3D miniband exciton. To obtain an idea of the physics behind this process, the field dependence of the absorption near the position of the 3D exciton ground state shall be investigated in some more detail. Figure 8 shows absorption spectra calculated for the 12/6-ML GaAs/AlAs superlattice between $F=1.25$ and 10 kV/cm. In Fig. 8(a) the broadening is the same as in Fig. 2(a), in Fig. 8(b) it is reduced to a FWHM equal to 2 meV. In

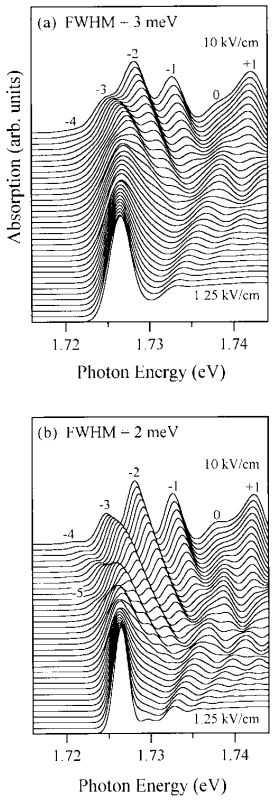

FIG. 8. Calculated field-dependent excitonic absorption spectra in the vicinity of the band-gap energy for the 12/6-ML GaAs/AlAs superlattice for two different values of the broadening parameter.

both plots, the structure due to the ground state of the 3D miniband exciton is clearly visible in the low-field limit, and remains nearly unaffected in its shape with increasing field, unless the field reaches a certain threshold value. At this point the 3D exciton decouples into the exciton resonances of the WS transitions. The threshold field obviously depends on the line broadening, since, as it is reduced, the linewidth is reduced. Therefore, in Fig. 8(b) the observation of WS peaks down to $\eta=-5$ is possible, whereas only levels down to $\eta=-3$ can clearly be identified in Fig. 8(a). Of course, the lower-index levels are also present in the more strongly broadened spectra of Fig. 8(a), but they cannot be resolved and thus merge together, forming the structure observed as the 3D miniband exciton. Obviously, the miniband absorption peak at small, but finite electric fields can be interpreted as being composed of low-order WS exciton peaks, which experience an absorption resonance when they cross the energetic position of the zero-field miniband exciton.

This behavior can be explained easily. The field-free exciton system has a discrete exciton ground state for a certain energy (for higher bound states, the same considerations can be used), which has a high probability density at $z=0$. As soon as an electric field is applied, the Coulomb potential becomes tilted, and the bound states transform to (possible) resonances of the system. The situation, however, is different from the bulk case (which leads to the excitonic FK effect), as the boundary conditions imposed by the finite bandwidths only allow for discrete states rather than an energy continuum with respect to the z direction. Therefore, an absorption resonance is only possible, if a (allowed) WS exciton

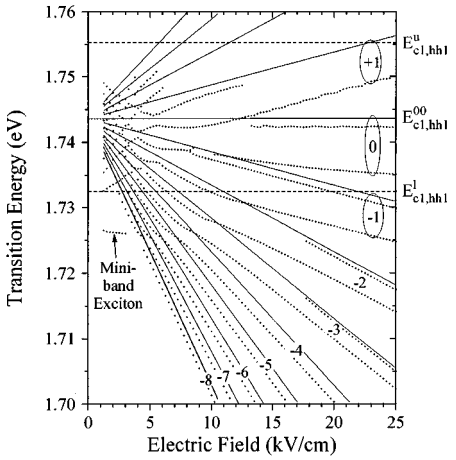

FIG. 9. Field dependence of the exciton absorption peak energies (dots) and single-particle WS transition (lines) for the 12/6-ML GaAs/AlAs superlattice.

level crosses the position of the zero-field ground state of the miniband exciton. This effect leads to a peak in the absorption at the position of the 3D miniband exciton for each WS level. The peaks merge together, when the distance between the WS levels becomes too small to be resolved, and the resonance of the 3D miniband exciton is formed. Similar to the single-particle case, this transition is *not* governed by an intrinsic property of the excitonic WS effect, such as the relation between WS level distance and exciton binding energy, but only by the external mechanisms leading to the broadening of the energy levels. Of course, the resonance effects become weaker as soon as the applied field exceeds the ionization field, given by

$$F_{\text{ion}}=\frac{R_x}{ea_x}=\frac{(\mu^*)^2e^5}{128\pi^3\epsilon_0^3\epsilon_r^3\hbar^4}\approx 4.3\ \text{kV/cm} \qquad (23)$$

(the explicit value is calculated for the 3D *hh* excitons of GaAs) so that the low-field limit may not be reachable in many experiments. This is the situation in our measurements plotted in Fig. 5(a), which start with a field value of $F=27$ kV/cm. Nevertheless, the decoupling of the miniband exciton feature into WS excitons is clearly visible, both in theory and experiment.

The resonance phenomenon also manifests itself in the binding energy of the WS excitons. In Fig. 9 the energies of the absorption peaks of the 12/6-ML GaAs/AlAs sample extracted from the calculated spectra of Fig. 2 are plotted as dots, and the single-particle WS transition energies as solid lines. In the high-field range, one clearly recognizes the ground-state exciton peaks for the negative WS transitions, and, for some of them, even the first excited states. From the positive transitions, only the $\eta=+1$ peak can be identified, the others are too weak or are obscured by the numerical discretization ''noise.'' In the low-field regime, rather than individual WS peaks the maxima of the FK oscillations are observed. It is interesting to note that in the intermediate-field (3.5–6 kV/cm) and -energy (1.735–1.745 eV) range, an indication of exciton anticrossings occurs, which was described by Dignam and Sipe.[14] These structures cannot unambiguously be identified, but in view of our above results

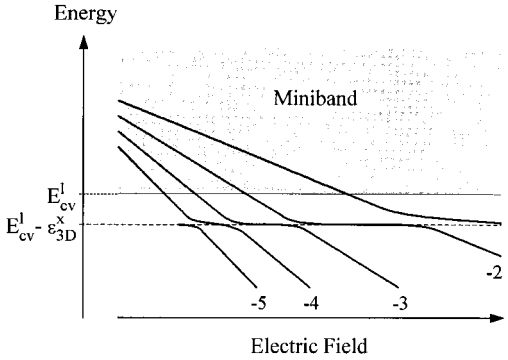

FIG. 10. Schematic picture of the exciton anticrossing behavior near the position of the zero-field miniband exciton in a superlattice.

and the results of Ref. 11 we tend to ascribe them to the interplay between WS transitions and FK oscillations, i.e., to effects of the varying oscillator strength rather than anticrossings between exciton levels.

We are interested now in the characteristic field dependence of the negative WS absorption peaks in the energy range below the single-particle miniband gap (<1.7324 eV). For this range, a serpentine shape of the peak positions in the vicinity of the miniband exciton energy is obtained, which corresponds to a strong enhancement of the WS exciton binding energy at the respective field values. This is a clear consequence of resonance with the zero-field exciton level, and results from the fact that a high exciton probability density at $z=0$ also yields a large expectation value of the Coulomb energy.

There is, however, a further interesting aspect. Consider, as an example, the ($\eta=-3$) transition. As it approaches the zero-field exciton position from low energies (high fields), it changes its energy with $-3eFd$, as expected from its transition index. After crossing the zero-field resonance, however, it continues according to $-4eFd$. Obviously, the resonant coupling with the zero-field exciton is accompanied by a change of the dipole moment of the electron-hole pair. Thus it actually causes a transformation between each two neighboring WS transitions. In another picture, this situation can be seen as follows (Fig. 10). When the ($\eta=-4$) transition approaches the zero-field exciton level from higher energies (low fields), it is ''captured'' by the zero-field exciton at its resonance position. At this point the WS exciton wave function receives a strong contribution from the zero-field exciton state, and, since the latter has a zero dipole moment, the mixed state loses part of its dipole moment and the field dependence of its energy is strongly weakened. Then, however, the ($\eta=-3$) WS exciton approaches from above, an anticrossing between the two excitons occurs, and the ($\eta=-3$) exciton replaces the ($\eta=-4$) exciton. During this process, the ($\eta=-4$) exciton loses one ''quantum'' of dipole moment and continues as the ($\eta=-3$) exciton. This situation is repeated for any negative WS transition. In this way the absorption resonance of the 3D miniband exciton is formed by a repeated anticrossing between the 2D WS excitons approaching its energetic position.

This behavior is completely independent of the actual values of the bandwidth and the exciton binding energies. Thus,

we disagree with the conclusion of Fox *et al.*,[15] who proposed the ratio between the exciton binding energy and the miniband width to be a criterion for the distinction between a ''multiple quantum well structure'' and a ''superlattice'' in electroabsorption experiments. The ''exciton localization'' effect, tending to move the electron and the hole closer to each other, can clearly alter the oscillator strengths of the WS transitions, but will not be able to suppress them. Instead, the relevant condition is the ratio between the spectral resolution (linewidth) and the combined miniband width, since the oscillator strengths of the WS transitions (excitons) decay rapidly, as soon as the transition lies outside the energy range of the combined miniband. If the experimental linewidth exceeds the combined miniband width, WS transitions other than the zero transition will be obscured by the spectral tails of the zero transition. This, however, is an effect which is entirely due to the behavior of the single-particle wave functions, and is not related to excitonic effects. Furthermore, it depends only on an ''extrinsic'' property of the system, the linewidth, which results from scattering processes and disorder, but not from a property of the WS ladder itself.[35]

To prove these conclusions, the results of Fox *et al.* will be analyzed. We choose the case for which the greatest amount of exciton localization effect is expected, i.e., the hh1-c1 miniband transitions of the most weakly coupled superlattice in their experiments. The sample is a 95 Å/35 Å $GaAs/Al_{0.3}Ga_{0.7}As$ superlattice with a calculated combined miniband width of 5.5 meV, which is less than both the 2D ($\varepsilon^x_{2D} \approx 8.3$ meV) and 3D ($\varepsilon^x_{3D} \approx 6.4$ meV) exciton binding energies. In the experimental results of Fox *et al.* (Fig. 5 of Ref. 15) an anticrossing-type behavior is observed both for hh and lh transitions, which is attributed to the ($\eta=0$) and ($\eta=1$) WS excitons by the authors. The anticrossing is explained by the suggestion that the (spatially indirect) ($\eta=-1$) WS exciton has a smaller binding energy than the ($\eta=0$) WS exciton. For small fields, this difference exceeds the electric-field energy eFd, and the ($\eta=-1$) exciton state has a higher energy than the ($\eta=0$) exciton, whereas, for high fields, the situation is reversed. The anticrossing should occur at the field value where eFd is just equal to the difference of the exciton binding energies. Further WS transitions are not observed, due to the proposed exciton localization mechanism.

In Fig. 11, the results of our calculations for the hh1-c1 transition are shown. The field values and the linewidth broadening (the FWHM is 3 meV) are chosen to be similar to the experimental values. As in experiment an anticrossing line shape around $F \approx 4$ kV/cm is obtained, and further WS transitions are not observed. According to the above discussion, however, the anticrossing behavior should be interpreted as taking place between the zero-field exciton state and the ($\eta=-1$) WS transition when approaching from low fields, and leading to ($\eta=-1$) and ($\eta=0$) WS excitons for higher fields. This conclusion is confirmed by the high-resolution calculations [Fig. 12(a)], which can resolve the ground state and, partly, also the first excited state of a couple of further WS excitons. The field dependence and the multiple anticrossings are exactly as described above, except for the fact that they also occur for excited exciton states, which were excluded from the above discussion. In particular, the transition from the miniband exciton feature to the WS excitons now takes place as soon as for the ($\eta=-3$) WS transition, due to the decreased spectral broadening. A comparison with the single-particle differential absorption spectra [Fig. 12(b)] further shows that the transition strengths in both plots decay within approximately the same energy range; i.e., the field and energy dependence of the exciton oscillator strengths is mainly due to the properties of the corresponding single-particle wave functions and only slightly affected by excitonic effects.

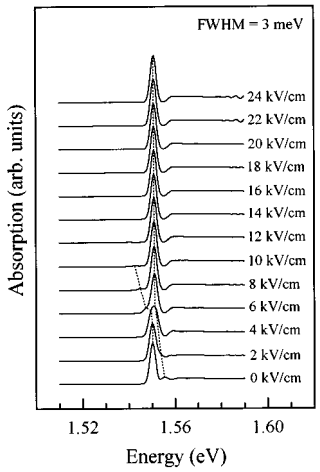

FIG. 11. Calculated excitonic electroabsorption spectra of the (95 Å/35 Å) $GaAs/Al_{0.3}Ga_{0.7}As$ superlattice discussed by Fox *et al.* (Ref. 15). The values of the electric field and the linewidth broadening have been chosen in agreement with the experimental results.

Thus, our conclusions deviate from those of Fox *et al.* in two aspects: First, we have shown that the anticrossing of the exciton peaks occurs between the 3D miniband exciton and the ($\eta=-1$) WS exciton rather than between two different WS excitons. In particular, there is no Coulomb-induced reversal of the natural sequence of WS transitions. Second, we demonstrated that the unobservability of higher WS transitions is not due to an exciton localization effect, but results from a combination of the fast decay of the single-particle transition strengths outside the miniband range, and the finite linewidth of the transitions. The other conclusions of Fox *et al.* are unaffected by these results. In particular, the description of the experiments in terms of a coupled two-well (n-well) model is correct, as long as a maximum of two (n) WS transitions can be resolved. Furthermore, the properties of the *zero-field* exciton itself, of course, tend toward those of a quasi-2D exciton, if the miniband width becomes smaller than the exciton binding energy.

VII. CONCLUSIONS

We computed the properties of excitons in the electroabsorption spectra of strongly coupled semiconductor superlattices, and compared them with single-particle calculations and experimental results. An excitonic theory is necessary for a correct description and interpretation of the spectra, since the electron-hole Coulomb interaction strongly alters the line shapes, but it is also an interesting problem on its own in view of the field-induced dimensionality transition

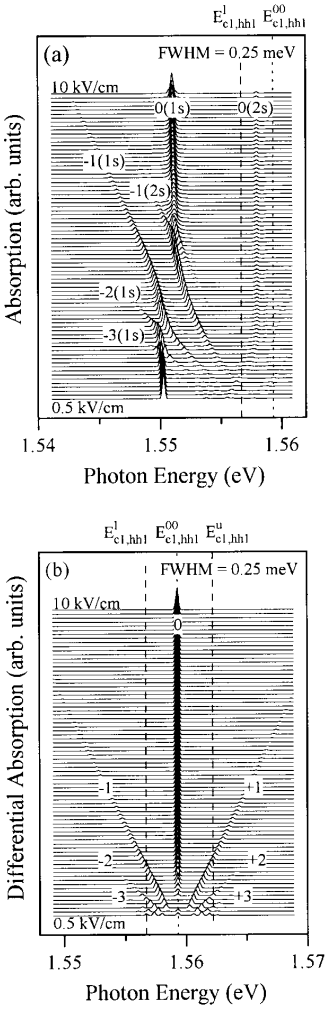

FIG. 12. High-resolution excitonic absorption spectra (a) and differential absorption spectra (b) for the 95-Å/35-Å $GaAs/Al_{0.3}Ga_{0.7}As$ superlattice. Dashed lines: combined miniband edges; dotted line: ($\eta=0$) single-particle transition.

(from 3D to 2D) of the system.

We used an approach leading to a system of integral equations for the eigenenergies and wave functions of the full exciton Hamiltonian in the effective-mass approximation. After discretization, the problem could be diagonalized numerically. In contrast to many previous approaches our calculations contain both bound and continuum states of the excitons, treated on an equal footing. Therefore, interaction between different bound states as well as between bound states and continua could be investigated.

An analysis of the absorption spectra over a wide range of fields has shown that, for samples with wide to moderate miniband widths, three different field regimes can be distinguished as in the single-particle picture: In the high-field regime one obtains a series of bound exciton states and an excitonic continuum for each WS transition. The binding energies and the shape of the absorption continuum reflect the 2D character of the excitons. For zero field, 3D M_0 and M_1 exciton absorption features are observed at the lower and the upper combined miniband edge, enclosing a flat absorption plateau in between. As the field is increased, miniband FK oscillations evolve at both miniband edges. In the intermediate-field regime an interference between WS transitions and FK oscillations occurs, consisting of FK-type modulations of the WS excitons, similar to the same effect obtained in the single-particle spectra. Remarkably, the properties of the absorption spectra are mostly determined by the properties of the single-particle states. In particular, the formation of FK oscillations is not suppressed by Coulomb effects, even if the oscillation width is much less than the exciton binding energy. The Coulomb forces, however, redistribute oscillator strength from higher to lower energies, leading to a strong asymmetry of the intensity of the structures between the lower and upper halves of the combined miniband.

Particular interest was devoted to a study of the field-induced dimensionality transition of the exciton states. Our calculations show that the bound states of the miniband exciton for small fields can be understood as resonances of the various WS excitons when crossing the respective energy position. The value of the field, where the decay of the miniband exciton into the WS excitons can be observed, depends on the linewidth of the transitions only, but not on the exciton binding energy. In no relevant case has an exciton localization mechanism, competing with the field-induced localization of the single-particle states, been found to be able to suppress WS transitions or to change their order. Even if the exciton binding energy exceeds the combined miniband width, a number of WS excitons in their natural sequence is obtained in high-resolution calculations, although lower-resolution calculations in agreement with experimental results seem to give evidence of the existence of a pair of WS excitons only. Therefore, we conclude that, in contradiction to previous assumptions, the ratio of miniband width and exciton binding energy is not an appropriate criterion for the distinction between a superlattice and a MQW structure in absorption experiments. In contrast, the relevant property is only the relation between the miniband width and the linewidth of the transitions.

ACKNOWLEDGMENTS

The author thanks G. H. Döhler, H. T. Grahn, K. H. Schmidt, and W. Geisselbrecht for many helpful discussions.

[1] E. E. Mendez, F. Agulló-Rueda, and J. M. Hong, Phys. Rev. Lett. **60**, 2426 (1988)

[2] P. Voisin, J. Bleuse, C. Bouche, S. Gaillard, C. Alibert, and A. Regreny, Phys. Rev. Lett. **61**, 1639 (1988).

[3] H. M. James, Phys. Rev. **76**, 1611 (1949).

[4] E. O. Kane, J. Phys. Chem. Solids **12**, 181 (1959).

[5] G. H. Wannier, Phys. Rev. **117**, 432 (1960).

[6] W. Franz, Z. Naturforsch. **13a**, 484 (1958); L.V. Keldysh, Zh. Éksp. Teor. Fiz. **34**, 1138 (1958) [Sov. Phys. JETP **34**, 788 (1958)].

[7] D. E. Aspnes and N. Bottka, *Electric-Field Effects on the Dielectric Function of Semiconductors and Insulators*, edited by R. K.

Willardson and A.C. Beer, Semiconductors and Semimetals, Vol. 9 (Academic, New York, 1972).
[8] C. Coriasso, D. Campi, C. Cacciatore, C. Alibert, S. Gaillard, B. Lambert, and A. Regreny, Europhys. Lett. **16**, 591 (1991).
[9] H. Schneider, A. Fischer, and K. Ploog, Phys. Rev. B **45**, 6329 (1992).
[10] K. H. Schmidt, N. Linder, G. H. Döhler, H. T. Grahn, K. Ploog, and H. Schneider, Phys. Rev. Lett. **72**, 2769 (1994).
[11] N. Linder, K. H. Schmidt, W. Geisselbrecht, G. H. Döhler, H. T. Grahn, K. Ploog, and H. Schneider, Phys. Rev. B **52**, 17 352 (1995).
[12] For very high fields the spatial extension of the WS states saturates to one superlattice period, i.e., a situation analogous to a multiple quantum-well structure is obtained.
[13] M. M. Dignam and J. E. Sipe, Phys. Rev. Lett. **64**, 1797 (1990).
[14] M. M Dignam and J. E. Sipe, Phys. Rev. B **43**, 4097 (1991).
[15] A. M. Fox, D. A. B. Miller, J. E. Cunningham, W. Y. Jan, C. Y. P. Chao, and S. L. Chuang, Phys. Rev. B **46**, 15 365 (1992).
[16] N. F. Johnson, J. Phys. Condens. Matter **2**, 2099 (1990).
[17] M. F. Pereira, Jr., I. Galbraith, and S. W. Koch, Phys. Rev. B **42**, 7084 (1990).
[18] P. Hilton, J. Goodwin, P. Harrison, and W. E. Hagston, J. Phys. A **25**, 5365 (1992).
[19] R. P. Leavitt and J. W. Little, Phys. Rev. B **42**, 11 784 (1990).
[20] H. Chu and Y.-C. Chang, Phys. Rev. B **36**, 2946 (1987).
[21] H. Chu and Y.-C. Chang, Phys. Rev. B **39**, 10 861 (1989).
[22] D. M. Whittaker, Phys. Rev. B **41**, 3238 (1990).
[23] D. M. Whittaker, Superlatt. Microstruct. **7**, 375 (1990).
[24] D. M. Whittaker, Europhys. Lett. **31**, 55 (1995).
[25] S. Glutsch, D. S. Chemla, and F. Bechstedt, Phys. Rev. B (to be published).
[26] S.-L. Chuang, S. Schmitt-Rink, D. A. B. Miller, and D. S. Chemla, Phys. Rev. B **43**, 1500 (1991).
[27] R. A. Smith, *Wave Mechanics of Crystalline Solids* (Chapman and Hall Ltd., London, 1961).
[28] R. Winkler, Phys. Rev. B **51**, 14 395 (1995).
[29] C. Hermann and C. Weisbuch, Phys. Rev. B **15**, 823 (1977).
[30] E. O. Kane, Phys. Rev. **180**, 852 (1969).
[31] I. Balslev, Solid State Commun. **52**, 351 (1984).
[32] F. Agulló-Rueda, J. A. Brum, E. E. Mendez, and J. M. Hong, Phys. Rev. B **41**, 1676 (1990).
[33] H. Haug and S.W. Koch, *Quantum Theory of the Optical and Electronic Properties of Semiconductors*, 3rd ed. (World Scientific, Singapore, 1994).
[34] U. Fano, Phys. Rev. **124**, 1866 (1961).
[35] The field-induced tunneling between the minibands and the Fano-type broadening are so small in any relevant case that they do not remarkably contribute to the linewidth.